Role of Surface Hydrophobic Residues in the Conformational Stability of Human Lysozyme at Three Different Positions[†,‡]

Jun Funahashi,[§] Kazufumi Takano,[§] Yuriko Yamagata,[||] and Katsuhide Yutani*[,§]

Institute for Protein Research, Osaka University, 3-2 Yamadaoka, Suita, Osaka 565-0871, Japan, and Graduate School of Pharmaceutical Sciences, Osaka University, Yamadaoka, Suita, Osaka 565-0871, Japan

Received July 6, 2000; Revised Manuscript Received September 12, 2000

ABSTRACT: To evaluate the contribution of the amino acid residues on the surface of a protein to its stability, a series of hydrophobic mutant human lysozymes (Val to Gly, Ala, Leu, Ile, Met, and Phe) modified at three different positions on the surface, which are located in the α-helix (Val 110), the *β*-sheet (Val 2), and the loop (Val 74), were constructed. Their thermodynamic parameters of denaturation and crystal structures were examined by calorimetry and by X-ray crystallography at 100 K, respectively. Differences in the denaturation Gibbs energy change between the wild-type and the hydrophobic mutant proteins ranged from 4.6 to −9.6 kJ/mol, 2.7 to −1.5 kJ/mol, and 3.6 to −0.2 kJ/mol at positions 2, 74, and 110, respectively. The identical substitution at different positions and different substitutions at the same position resulted in different degrees of stabilization. Changes in the stability of the mutant proteins could be evaluated by a unique equation considering the conformational changes due to the substitutions [Funahashi et al. (1999) *Protein Eng. 12,* 841−850]. For this calculation, secondary structural propensities were newly considered. However, some mutant proteins were not adapted to the equation. The hydration structures around the mutation sites of the exceptional mutant proteins were affected due to the substitutions. The stability changes in the exceptional mutant proteins could be explained by the formation or destruction of the hydration structures. These results suggest that the hydration structure mediated via hydrogen bonds covering the protein surface plays an important role in the conformational stability of the protein.

Generally, the surface residues of a protein are widely regarded as tolerant of substitution. Because exposed sites in the native state would also be exposed in the denatured state, it seems that the substitution does not affect the protein stability. The energetic consequences of substitutions on the surface of a protein have been reported to be smaller than the effects of substitutions in the interior (*1*−*3*). These energetic changes, however, are not negligible, and while on the average they are somewhat smaller, they are comparable in magnitude to the energetic effects of changes in the core of the protein (*4*). In fact, several mutagenesis studies have shown that a substitution on the surface of a protein affects its stability variously (*4*−*10*). In practice, the substitutions at solvent-exposed positions might lead to changes in the contributions of the stabilization factors to protein stability, such as the hydrophobicity, electrostatic interaction, hydrogen bonds, conformational entropy, propensity scale of the secondary structure, and hydration structure. Pakula and Sauer (*5*) have reported that when a hydrophobic amino acid is substituted into a hyperexposed site on the surface, the protein can be destabilized with an increase in the hydrophobicity, showing the "reverse hydrophobic effect". In contrast to this destabilizing effect, the stabilizing effect has also been observed by other groups (*6*, *11*). These results suggest that the effects of the substitutions at the surface of proteins on the conformational stability would change variously, depending on the environment of the mutation sites. The various contributions of the surface residues to the conformational stability of a protein, however, remain to be extensively and quantitatively examined.

To understand basically and quantitatively the role of surface residues, systematic surveys are useful. In this study, we focused on the hydrophobic substitutions at various positions on the surface of a protein. These substitutions would not cause changes in the contribution of the electrostatic interaction and the hydrogen bonds of the mutation site to protein stability. This may give us an essential understanding of the role of surface residues in the conformational stability of a protein. Human lysozyme (130 residues) is a good model protein for the physicochemical study of systematic mutants (*12*). Three different positions (Val 2, Val 74, and Val 110) on the surface of human lysozyme, examined in this paper, are located in different secondary structures (*β*-sheet, loop, and α-helix, respectively), and 72, 75, and 71% of the residues are exposed,

[†] This work was supported in part by Fellowships from the Japan Society for the Promotion of Science for Young Scientists (J.F. and K.T.) and by a Grant-in-Aid for special project research from the Ministry of Education, Science and Culture of Japan (Y.Y. and K.Y.).

[‡] Coordinates have been deposited in the Brookhaven Protein Data Bank as PDB file names 1GAY (V2G), 1GAZ (V2I), 1GB0 (V2L), 1GB2 (V2M), 1GB3 (V2F), 1GB5 (V74G), 1GB6 (V74I), 1GB7 (V74L), 1GB8 (V74M), 1GB9 (V74F), 1GBO (V110G), 1GBW (V110I), 1GBX (V110L), 1GBY (V110M), and 1GBZ (V110F).

* To whom correspondence should be addressed. Telephone: +81-6-6879-8615. Fax: +81-6-6879-8616. E-mail: yutani@protein.osaka-u.ac.jp.

[§] Institute for Protein Research.

[||] Graduate School of Pharmaceutical Sciences.

[1] Abbreviations: ASA, accessible surface area; DSC, differential scanning calorimetry; rms, root-mean-square; ΔC_p, heat capacity change; ΔG, Gibbs energy change; ΔH, enthalpy change; T_d, denaturation temperature.

10.1021/bi0015717 CCC: $19.00
Published on Web 11/04/2000

Table 1: X-ray Data Collection and Refinement Statistics for Mutant Human Lysozymes

	data collection								refinement					
	cell dimensions (Å)			resolution	measured	independent	complete-	R_{merge}		solvent	resolution		complete-	
	a	*b*	*c*	(Å)	reflections	reflections	ness (%)	(%)[a]	atoms	atoms	(Å)	reflections	ness (%)	R_{factor}[b]
						Wild-Type								
	56.18	61.28	32.64	1.8	28942	10014	90.7	7.2	1313	284	8−1.8	9302	86.2	0.172
						Val 2 Mutants								
G	55.96	62.50	31.99	1.8	29322	10116	92.1	7.4	1331	305	8−1.8	9386	87.3	0.169
I	56.41	60.99	32.96	1.8	32569	10339	93.3	4.7	1331	301	8−1.8	9995	91.7	0.168
L	56.40	61.46	32.57	1.8	32720	10498	95.4	5.9	1274	244	8−1.8	10117	93.2	0.184
M	56.42	61.73	32.22	1.8	33326	10719	96.8	7.7	1321	291	8−1.8	10256	95.1	0.176
F	56.49	61.33	32.38	1.8	33756	10661	97.3	7.7	1300	267	8−1.8	10398	96.5	0.183
						Val 74 Mutants								
G	56.53	61.04	32.74	1.8	33762	10271	92.7	6.5	1322	296	8−1.8	9913	91.4	0.178
A	56.65	61.90	32.33	1.8	27632	10021	90.9	6.6	1290	263	8−1.8	9764	89.7	0.164
I	56.48	61.36	32.56	1.8	27589	9952	90.2	7.1	1314	284	8−1.8	9254	85.4	0.159
L	56.18	61.02	32.77	1.8	16160	7842	67.0	10.2	1299	269	8−1.8	6469	60.0	0.168
M	56.39	61.19	32.70	1.8	28333	9669	87.6	6.6	1312	282	8−1.8	9048	83.5	0.158
F	56.23	61.47	32.69	1.8	31676	10393	95.1	6.2	1328	295	8−1.8	10072	92.8	0.181
						Val 110 Mutants								
G	56.33	61.10	32.55	1.8	26772	9322	87.3	6.7	1306	280	8−1.8	8752	81.3	0.169
A	56.33	60.95	32.91	1.8	30733	10316	94.6	9.0	1312	285	8−1.8	9824	90.4	0.189
I	56.42	60.50	33.03	1.8	21988	8482	76.7	9.9	1292	262	8−1.8	7553	69.3	0.163
L	56.37	61.35	32.49	1.8	24971	9034	82.0	7.5	1341	311	8−1.8	8090	74.9	0.151
M	56.82	60.96	33.03	1.8	11819	8483	76.0	10.9	1304	274	8−1.8	7154	65.1	0.166
F	56.51	60.28	32.40	1.8	26275	9479	86.6	6.6	1302	269	8−1.8	8591	81.0	0.178

[a] $R_{merge} = 100\sum|I - \langle I\rangle|/\langle I\rangle$. [b] $R_{factor} = \sum||F_o| - |F_c||/\sum|F_o|$. The crystal structure of Val → Ala mutants were reanalyzed at 100 K.

respectively. At these three Val positions, a series of hydrophobic mutants replaced with Gly, Ala, Leu, Ile, Met, or Phe were constructed. The thermodynamic parameters for denaturation of the mutant proteins were determined using differential scanning calorimetry (DSC), and the crystal structures were determined by X-ray analysis at 100 K. At low temperatures, cryogenic crystal structures are expected to reveal the details of hydration structures due to the decrease in thermal vibrations (*13, 14*). The role of surface hydrophobic residues in the conformational stability of a protein will be discussed in relation to the hydration structures on the protein surface.

MATERIALS AND METHODS

Mutant Proteins. Mutagenesis, expression, and purification of mutant human lysozymes were performed as described (*12*). The concentration of the mutant proteins was spectrophotometrically determined using $E^{1\%}$ (1 cm) = 25.65 at 280 nm (*15*).

Differential Scanning Calorimetry (DSC). Calorimetric measurements and data analyses were carried out as described (*12*). For the measurements, a DASM4 adiabatic microcalorimeter equipped with an NEC personal computer was used. The sample buffer for measurements was 0.05 M Gly-HCl (pH 2.5−3.3). Data analysis was done using Origin software (MicroCal, Inc., Northampton, MA).

X-ray Structural Analysis. Mutant human lysozymes were crystallized as described (*12, 16*). All crystals belong to space group $P2_12_12_1$ with a crystal form identical to that of the wild-type and of most mutant proteins.

All intensity data were collected at 100 K by the osillation method on a Rigaku R-AXIS IV imaging plate mounted on a Rigaku RU300 rotating anode X-ray generator. Their structures were solved by the isomorphous method. The structures were refined with the program X-PLOR (*17*) as described (*12, 16*). Detection of solvent molecules was done using the program FLAPPER (Fujii, S., unpublished). The criteria for selecting the solvent molecules were to have hydrogen bonding geometry contacts of 2.4−3.5 Å (except for one peak assigned to a Na^+, which binds to carbonyl oxygen and water molecules with contacts of 2.1−2.3 Å) with protein atoms or with the existing solvent, excluding contacts to carbon atoms within 3.2 Å, to have temperature factors less than 45 Å^2, and to have electron densities of more than the 2.5σ level in $F_o - F_c$ maps, as described by Takano et al. (*12*).

Although the data sets for the wild-type, V2A, V74A, and V110A had been collected and their structures had been solved at 283 K (*18*), their data were recollected and resolved at 100 K except for V2A. The crystal of V2A could not be grown under the same conditions described by Takano et al. (*18*).

Calculation of ASA Values. The accessible surface area (ASA) values of the proteins were calculated by the procedure of Connolly (*19*) with a probe radius of 1.4 Å as previously described (*20, 21*). The ASA values of the denatured state were calculated using an actual polypeptide of five residues including the mutation site in the middle (*18, 22*).

RESULTS

Structures of Mutant Human Lysozymes. All structures of mutant proteins could be determined by X-ray analysis and were essentially identical with the wild-type structure. The data collection and refinement statistics for a series of mutant human lysozymes are summarized in Table 1. As described above, all intensity data were collected at 100 K. Figure 1a,c shows the rms deviations and the B-factors for each residue for the main-chain atoms between the wild-type structures at 100 and 283 K (*12*), respectively. The wild-type structure at 100 K seems to be essentially the same fold as the wild-type structure at 283 K. The residues greatly shifted

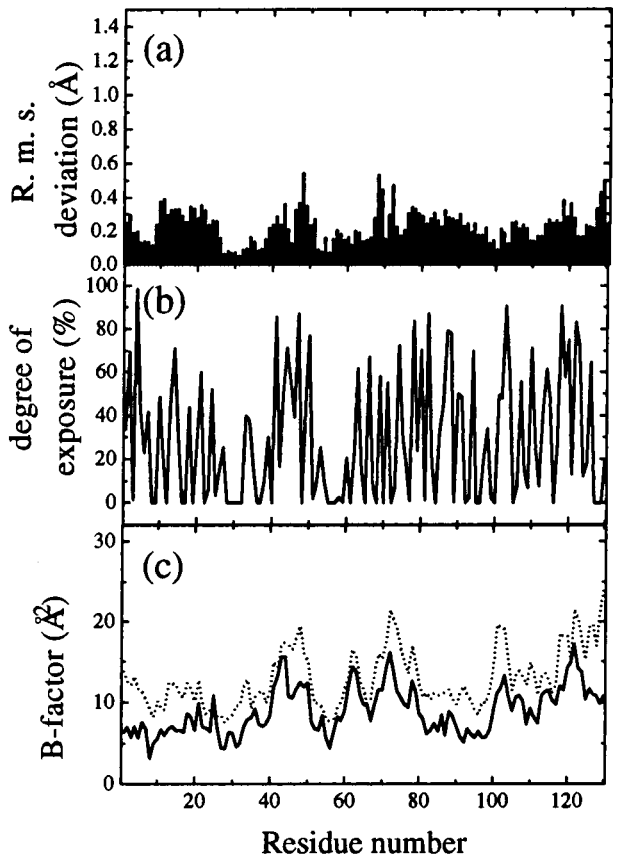

FIGURE 1: The differences between the structures of the wild-type human lysozyme at 100 and 283 K: (a) RMSDs for the main-chain atoms; (b) the rate of exposure of the wild-type structure at 100 K; (c) B-factor for the wild-type structure at 100 K (solid) and 283 K (dotted).

corresponding to those at the exposed site (Figure 1b). The B-factors for the wild-type protein at 100 K were significantly smaller than those at 283 K because thermal vibrations would decrease at lower temperature. The B-factors for the observed hydration water molecules at 100 K, especially water molecules which are located close to the protein, were also smaller than those at 283 K. Most of the water molecules which are located close to the protein formed a hydrogen bond with protein atoms. They were also observed at almost the same positions in other mutant structures. The aggregates of hydration water molecules were linked together via hydrogen bonds and connected through the hydrogen bonds mediated by polar atoms of the protein.

Figure 2 shows the Connolly surface of the residues which are located around the mutation site, position 2. The C^{β} atom of each substituted residue (except for Gly) was located at almost the same position as the wild-type protein. As a result, they extended their side chains in the same direction as the wild-type protein. Because the substituted hydrophobic residues were attached closely to the surface of a protein, the accessible surface area of the substituted residues in the native structures considerably decreased compared with their surface area in the extended structures. The same trends were observed at positions 74 and 110.

Stability of Mutant Human Lysozymes. DSC measurements of mutant human lysozymes were carried out in the acidic region (pH 2.5−3.3) where the heat denaturation of human lysozyme is completely reversible. Table 2 shows the denaturation temperatures (T_d), the calorimetric enthalpies (ΔH_{cal}), and the van't Hoff enthalpies (ΔH_{vH}) of each measurement for the mutant proteins. The T_d values are sensitive to changes in pH and increased linearly with increasing pH for all the proteins examined. The thermodynamic parameters for denaturation as a function of temperature were calculated using the following equations:

$$\Delta H(T) = \Delta H(T_d) - \Delta C_p(T_d - T) \quad (1)$$

$$\Delta S(T) = \Delta H(T_d)/T_d - \Delta C_p \ln(T_d/T) \quad (2)$$

$$\Delta G(T) = \Delta H(\mathrm{T}) - T\Delta S(T) \quad (3)$$

where the ΔC_p values are assumed to be independent of temperature between 20 and 80 °C (*23*). Table 3 shows the thermodynamic parameters of denaturation at a constant temperature, 64.9 °C, and at pH 2.7 calculated using the above equations to compare thermodynamic parameters among mutant proteins under the same conditions. The heat capacity changes (ΔC_p) in denaturation were obtained from the slopes of the plot of ΔH_{cal} vs T_d. The changes in denaturation Gibbs energy ($\Delta\Delta G$) between the wild-type and the mutant proteins substituted at the positions of 2, 74, and 110 ranged from 4.6 to −9.6 kJ/mol, 2.7 to −1.5 kJ/mol, and 3.6 to −0.2 kJ/mol, at pH 2.7, respectively. Identical substitution at different positions and different substitutions at the same position resulted in different degrees of destabilization or stabilization. For instance, the mutant proteins of Val → Gly substitution at positions 2, 74, and 110 were destabilized, slightly destabilized, and stabilized, respectively, compared with the wild-type protein.

The denaturation enthalpy change (ΔH) of the mutant protein examined at 64.9 °C and pH 2.7 ranged from 370 to 484 kJ/mol; that of the wild-type protein was 477 kJ/mol (Table 3). The ΔH of most mutant proteins was lower than that of the wild-type protein, even if some of them were more stable than the wild-type protein. This trend was consistent with the other mutant human lysozymes substituted mainly at buried positions (*12, 16, 18, 20, 21, 24*−*28*). The determination of ΔH values for mutant proteins with DSC must be important for understanding the mechanism of protein stabilization. In this study, a correlation between the changes in ΔH value and the structural features was not found. For example, the ΔH value of V74I was the smallest among the mutants in this study, 370 kJ/mol, while that of the wild-type protein was 477 kJ/mol (Table 3). This unfavorable enthalpy term might be compensated by the favorable entropy term because this mutant protein was stabilized by 1.9 kJ/mol due to the substitution. These quite large changes in the entropy and enthalpy terms might be caused by the change in structural features, but the structural change in this mutant was quite small. The average of the rms deviation for the main-chain atoms of each residue between V74I and the wild-type protein was within 0.3 Å at all positions.

DISCUSSION

Estimation of the Stabilities of the Mutant Proteins Substituted at Three Different Exposed Positions. It has been reported that substitutions even at the surface of the protein often affect the conformational stability (*4, 9, 29, 30*). To

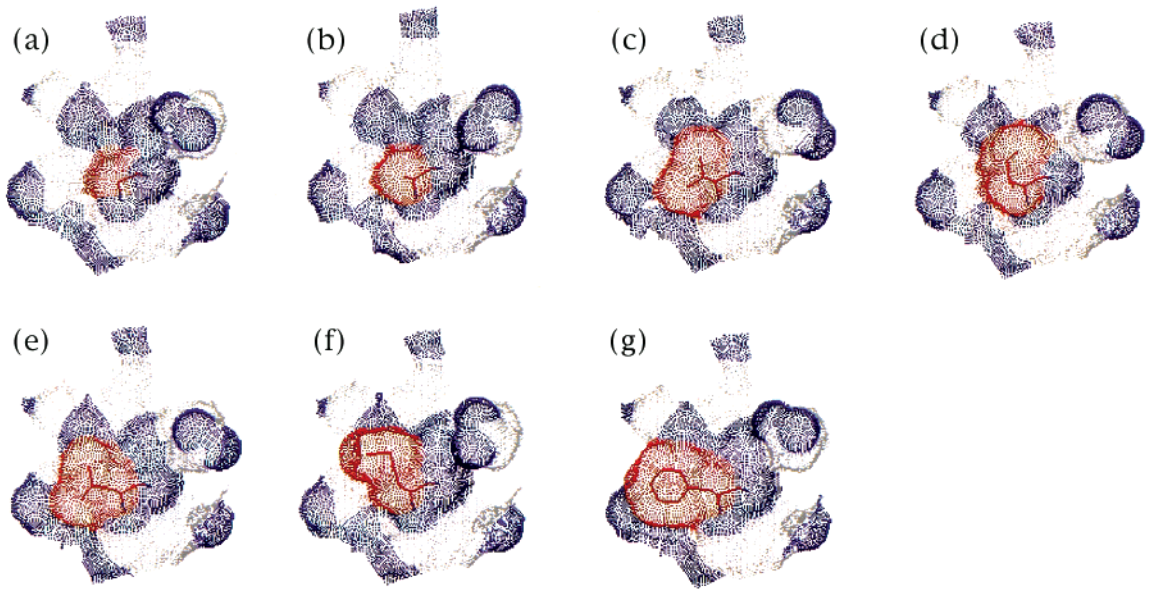

FIGURE 2: The Connolly surface (probe 1.4 Å) of the residues in the vicinity of the position 2. Blue, gray, and red dots represent the Connolly surface of the polar atoms, the nonpolar atoms, and that of the side chain of the substituted residue, respectively. The red lines represent the substituted residues at position 2. (a) V2G; (b) V2A; (c) wild-type (Val at position 2); (d) V2I; (e) V2L; (f) V2M; (g) V2F.

Table 2: DSC Data for Denaturation of Mutant Human Lysozymes at Different pHs

	position 2				position 74				position 110			
residue	pH	T_d (°C)	ΔH_{cal} (kJ/mol)	ΔH_{vH} (kJ/mol)	pH	T_d (°C)	ΔH_{cal} (kJ/mol)	ΔH_{vH} (kJ/mol)	pH	T_d (°C)	ΔH_{cal} (kJ/mol)	ΔH_{vH} (kJ/mol)
Gly	2.65	56.63	400	397	2.53	61.28	452	448	2.60	64.60	418	460
	2.83	59.46	417	415	2.78	65.50	481	469	2.73	67.11	435	477
	3.08	63.75	439	435	2.95	68.71	506	498	2.94	70.59	460	498
	3.19	65.70	452	444	3.09	70.82	519	506	3.11	73.44	481	527
	3.40	69.03	469	460	3.30	74.04	540	536	3.30	76.63	510	544
Ile	2.50	65.06	452	477	2.67	66.07	376	431	2.53	64.89	448	460
	2.70	67.98	477	502	2.80	68.29	387	448	2.70	67.27	464	477
	2.92	72.23	498	527	3.00	71.67	404	469	2.90	70.93	490	498
	3.13	75.47	523	552					3.13	74.86	515	527
									3.23	76.82	531	544
Leu	2.49	61.34	440	444	2.50	62.35	419	444	2.50	61.92	440	444
	2.70	64.55	456	461	2.70	65.28	435	469	2.70	65.02	452	456
	3.05	70.39	486	490	2.83	67.51	448	481	2.82	67.01	465	469
					3.05	71.61	469	502	3.03	70.53	481	486
					3.15	73.32	477	515	3.25	74.52	507	515
Met	2.52	60.62	444	444	2.50	63.42	448	473	2.48	62.80	456	481
	2.73	64.55	469	469	2.70	66.86	473	502	2.70	66.34	477	502
	2.94	68.26	494	498	2.83	69.38	490	519	2.85	69.11	494	523
	3.09	70.56	510	515	3.10	73.23	515	544	3.06	72.79	515	540
	3.31	74.24	531	531	3.20	74.95	523	557				
Phe	2.68	61.97	444	448	2.68	63.65	452	456	2.72	65.11	423	461
	2.87	65.05	460	469	2.84	66.32	469	477	2.80	66.29	431	469
	3.09	68.60	485	494	3.10	70.50	490	494	3.04	70.49	461	502
	3.22	71.22	506	510	3.23	72.44	502	510				
					3.40	75.60	519	523				

estimate the intrinsic effect of the substitution on the surface of a protein on the conformational stability, it is necessary to subtract the effect of other already-established stabilization factors due to the substitutions, such as hydrophobic effects, from the changes in mutant stability. Amino acid substitutions also change the extent of contributions of the stabilization factors to protein stability due to the conformational changes (*18*).

The stabilization factors have been assumed and examined by mutagenesis studies (*31*−*40*). Recently, it has been proposed that the stability of each mutant human lysozyme is represented by a unique equation, considering the conformational changes due to the mutations (*21*). In the study, changes in the hydrophobic effect, conformational entropy, hydrogen bonding, and water molecule introduced in the interior of a protein were considered as the stabilization factors. The difference in denaturation Gibbs energy between the wild-type and mutant proteins ($\Delta\Delta G$) is expressed by eq 4 (*21*).

$$\Delta\Delta G = \Delta\Delta G_{HP} + \Delta\Delta G_{conf} + \Delta\Delta G_{HB} + \Delta\Delta G_{H_2O} \quad (4)$$

where $\Delta\Delta G_{HP}$, $\Delta\Delta G_{conf}$, $\Delta\Delta G_{HB}$, and $\Delta\Delta G_{H_2O}$ represent the changes in ΔG due to the hydrophobic effect, the confor-

Table 3: Thermodynamic Parameters for Denaturation of Mutant Human Lysozymes at the Denaturation Temperature (64.9 °C) of the Wild-Type Protein at pH 2.7

	position 2				position 74				position 110			
residue	T_d (°C)	ΔC_p[a] (kJ/mol K)	ΔH (kJ/mol)	$\Delta\Delta G$ (kJ/mol)	T_d (°C)	ΔC_p[a] (kJ/mol K)	ΔH (kJ/mol)	$\Delta\Delta G$ (kJ/mol)	T_d (°C)	ΔC_p[a] (kJ/mol K)	ΔH (kJ/mol)	$\Delta\Delta G$ (kJ/mol)
Gly	57.4 ± 0.1	5.5 ± 0.1	446 ± 1	−9.6	64.2 ± 0.2	6.9 ± 0.2	477 ± 1	−0.9	66.5 ± 0.1	7.6 ± 0.3	418 ± 1	2.0
Ala[b]	60.3 ± 0.2	6.5 ± 0.5	468 ± 4	−6.3	63.8 ± 0.1	6.2 ± 0.4	476 ± 2	−1.5	66.4 ± 0.4	5.2 ± 0.4	484 ± 2	2.2
Val (WT)	64.9 ± 0.5	6.6 ± 0.5	477 ± 4	0.0	64.9 ± 0.5	6.6 ± 0.5	477 ± 4	0.0	64.9 ± 0.5	6.6 ± 0.5	477 ± 4	0.0
Ile	68.3 ± 0.3	6.6 ± 0.5	452 ± 2	4.6	66.6 ± 0.1	5.0 ± 0.1	370 ± 1	1.9	67.6 ± 0.2	6.9 ± 0.1	447 ± 1	3.6
Leu	64.7 ± 0.1	5.1 ± 0.1	458 ± 1	−0.2	65.5 ± 0.3	5.3 ± 0.1	433 ± 1	0.8	65.1 ± 0.2	5.4 ± 0.2	454 ± 1	0.3
Met	63.9 ± 0.2	6.5 ± 0.1	471 ± 1	−1.3	66.9 ± 0.3	6.6 ± 0.2	458 ± 1	2.7	66.5 ± 0.1	5.9 ± 0.1	468 ± 1	2.2
Phe	62.2 ± 0.2	6.8 ± 0.4	461 ± 1	−3.6	64.0 ± 0.2	5.6 ± 0.1	459 ± 1	−1.2	64.7 ± 0.1	7.1 ± 0.1	421 ± 1	−0.2

[a] ΔC_p was obtained from the slope of ΔH vs T_d. [b] Takano et al. (*12*).

mational entropy of the substituted residue, the formation and removal of hydrogen bonding, and the introduction of water molecules, respectively. Each $\Delta\Delta G$ can be expressed with each parameter in terms of the conformational change (eqs 5−8).

$$\Delta\Delta G_{HP} = 0.178\Delta\Delta ASA_{NP} - 0.013\Delta\Delta ASA_P \quad (5)$$

$$\Delta\Delta G_{conf} = -T\Delta\Delta S_{conf} \quad (6)$$

$$\Delta\Delta G_{HB} = 15.53\sum r_{HB}^{-1} \quad (7)$$

$$\Delta\Delta G_{H_2O} = -7.79\Delta N_{H_2O} \quad (8)$$

where ΔASA_{NP} and ΔASA_P represent the difference in the ASA of nonpolar and polar atoms of all residues in a protein due to denaturation, respectively; $\Delta\Delta ASA$ means the difference between the ΔASAs of the wild-type and mutant proteins; S_{conf} is the conformational entropy defined by Doig and Sternberg (*41*); r_{HB} is the length of the hydrogen bonds; and ΔN_{H_2O} is changes in the number of water molecules introduced by substitutions (*21*). By the fitting of the data obtained from changes in stability and structure for mutant human lysozymes substituted at various positions to eq 4, each parameter for the stabilization factor has been estimated (*21*, *26*). The units of the coefficients in eqs 5, 7, and 8 are 0.178 kJ·mol^{-1}·Å^{-2}, −0.013 kJ·mol^{-1}·Å^{-2}, 15.53 kJ·Å·mol^{-1}, and −7.79 kJ/mol, respectively.

In this study, the three different positions which are located in different structural environments (α-helix, β-sheet, and loop) were substituted with Gly, Ala, Val, Leu, Ile, Met, and Phe. Each amino acid residue has a characteristic intrinsic propensity to populate the secondary structure conformation (*42*). Therefore, the stabilization factors concerning the propensity of the secondary structure ($\Delta\Delta G_{pro}$) should be added to eq 4 as follows:

$$\Delta\Delta G = \Delta\Delta G_{HP} + \Delta\Delta G_{conf} + \Delta\Delta G_{HB} + \Delta\Delta G_{H_2O} + \Delta\Delta G_{pro} \quad (9)$$

$$\Delta\Delta G_{pro} = \alpha\Delta pro_{[\alpha]} + \beta\Delta pro_{[\beta]} \quad (10)$$

where $pro_{[\alpha]}$ and $pro_{[\beta]}$ are the α-helix and the β-sheet propensities, respectively, of the residue defined by Chou and Fasman (*43*) (revised by Koehl and Levitt (*44*)). The parameters (α, β) in eq 10 represent the contribution of the conformational preferences of amino acid residues to the secondary structure. A least-squares fit of the $\Delta\Delta G_{pro}$ in eq 10 to the $[\Delta\Delta G - (\Delta\Delta G_{HP} + \Delta\Delta G_{conf} + \Delta\Delta G_{HB} + \Delta\Delta G_{H_2O})]$ values using the stability/structure database of the mutant human lysozymes examined in our previous studies (*12*, *16*, *18*, *20*, *21*, *24*−*26*, *28*) gave $\alpha = 5.07$ and $\beta = 2.31$ kJ/mol. This means that the substitution by the residues observed more frequently on the secondary structure contributes more strongly to the protein stability. For example, the Val to Ala substitution in the α-helix stabilizes the mutant protein by 2.9 kJ/mol, and the same substitution in the β-sheet destabilizes it by 1.7 kJ/mol. There was a good correlation between the experimental value ($\Delta\Delta G_{exp}$) and the estimated value ($\Delta\Delta G_{est}$) using eq 9 (SD = 2.7 kJ/mol; Figure 3). In this analysis, the mutant proteins examined in this study were not included.

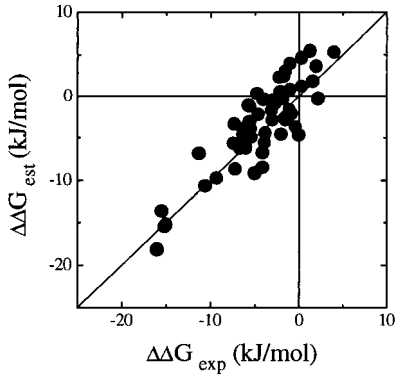

FIGURE 3: The results of the fitting using 54 mutant human lysozymes to obtain the parameters of eq 10. They are I23V, I56V, I59V, I89V, I106V (*12*); Y20F, Y38F, Y45F, Y54F, Y63F, Y124F (*16*); V2A, V74A, V93A, V99A, V100A, V110A, V121A, V125A (*18*); I23V-3s, I56V-3s, I89V-3s, I106V-3s, V2A-3s, V74A-3s, V110A-3s, V121A-3s, V125A-3s (*20*); I56L, I56M, I59M, I59L, I59S, I59T (*21*); I23A, I56A, I59A, I89A, I59G, I106A (*24*); S21A, S36A, S51A, S61A, S80A (*25*); T11A, T11V, T40A, T40V, T43A, T43V, T52A, T70V (*26*); I56T (*28*). The solid line represents $y = x$.

The $\Delta\Delta G$ values of a series of the mutant proteins substituted at the exposed positions can be estimated using the parameters of eq 9 and the structural information for mutant proteins obtained in this study. In this case, $\Delta\Delta G_{HB}$ and $\Delta\Delta G_{H_2O}$ can be assumed to be zero. ΔS_{conf} values were corrected corresponding to the degree of exposure of the substituted residue calculated from the crystal structure of each mutant. Figure 4 shows a correlation between the experimental $\Delta\Delta G$ and the estimated $\Delta\Delta G$ for mutant human lysozymes examined in this study. The estimated value agreed roughly with the experimental value with a few exceptions. The exceptions were V2G and V2F, which were

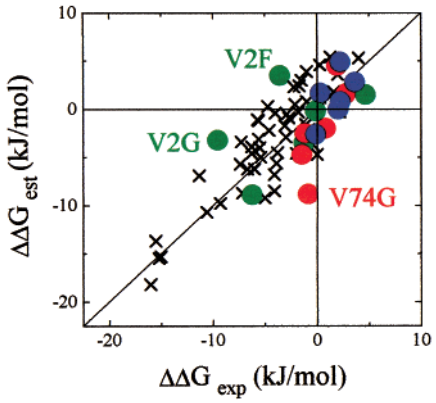

FIGURE 4: The relation between the experimental and estimated $\Delta\Delta G$ for the Val 2 (green circle), 74 (red circle), and 110 (blue circle) mutants. The cross symbol represents the same data for the mutant proteins in Figure 3.

more destabilized by 6.4 and 7.1 kJ/mol than the estimated $\Delta\Delta G$, respectively, and V74G which was more stabilized by 7.9 kJ/mol. In addition, the estimated $\Delta\Delta G$ tended to be lower than the experimental $\Delta\Delta G$.

Statistical α-helix and β-sheet propensity scales derived by Chou and Fasman (*43*) have been revised by Koehl and Levitt (*44*). The estimated stability of Val 110 mutants (Figure 4, blue circles) had a good correlation with the experimental stability, suggesting that the statistical propensity scale of the α-helix is quite useful for estimating the conformational stability of a protein. In fact, the correlation between the helix propensity scales of amino acids determined from different model peptide systems (*45*, *46*) and different mutant proteins (*29*, *47*) is in some cases quite good. In contrast to the helix propensity scale, the statistical β-sheet propensity scale seems to be different from those derived from experimental studies (*48*−*51*). In the present case, the estimated stability of Val 2 mutants using the statistical propensity scale also had good correlation with the experimental stability (Figure 4, green circles) except for V2G and V2F.

Table 4 lists the contribution of each factor to the mutant stabilities. The changes in stability were attributed mainly to $\Delta\Delta G_{HP}$. This indicates that the hydrophobic effect is one of the important stabilizing factors even if the residues are located on the surface. Compared with the hydrophobic effect, the contribution of the propensity of the secondary structure to protein stability was small but never negligible. Considering the propensity of the secondary structure of each substituted residue, the estimated $\Delta\Delta G$ value for mutant proteins substituted at positions 2, 74, and 110 agreed well with their experimental $\Delta\Delta G$, although these positions are located in different secondary structures, the β-sheet, loop, and α-helix, respectively. However, the deviation between both $\Delta\Delta G$ values was larger than the experimental errors of maximally 0.7 kJ/mol. This indicates that the difference between them contains the contribution of other factors to protein stability, which are not considered in the present calculation, such as changes in the hydration.

Hydration Structure around the Mutation Sites. The change in hydration structure due to mutations would be one of the factors which should be considered to elucidate the role of surface residues. Several hydration water molecules interact with each other via hydrogen bonds and form aggregates of various shapes and dimensions. The hydration water molecules composing the oligomers are in van der Waals contact with carbon atoms of hydrophobic residues, and the oligomers shield the hydrophobic side chains from the bulk solvent in the structure of trypsin (*14*). Thus, even the hydrophobic substitutions affect the hydration structure around the mutation site, resulting in changes in the conformational stability of a protein.

Figure 5 shows the hydration structure around positions 2 and 74. Red and blue dots represent the van der Waals surface of the substituted residue and water molecules, respectively. Many water molecules have interacted with protein atoms and each other via hydrogen bonds, covering the Val 2 residue (Figure 5a). The average B-factor for these water molecules displayed in Figure 5a was 23.8 Å^2. Due to the Val to Gly substitution, two water molecules were introduced in the space occupied by Val in the wild-type structure (Figure 5b). These new water molecules formed a different network of hydrogen bonds and destroyed the hydration structure. The side chain of Phe 2 also destroyed the network around Val 2 in the wild-type protein (Figure 5c). The unexpected destabilization of V2G and V2F (Figure 4) might be caused by the destruction of the hydration structures.

Around Val 74, the hydration structure was less rigid. The average B-factor for water molecules displayed in Figure 5d was 33.1 Å^2. In the case of V74G, the new water molecules introduced by the substitution formed a network via hydrogen bonds (Figure 5e). This would explain why V74G was more stabilized than expected. In contrast with V2F, the side chain of Phe 74 did not destroy the hydration structure observed in the wild-type structure (Figure 5f). The difference between $\Delta\Delta G_{exp}$ and $\Delta\Delta G_{est}$ of V74F was small.

In contrast, layers of water molecules interacting with each other and with protein atoms covered the area around position 110 of the Val 110 mutants. The layers of the hydrated water molecules around position 110 were somewhat apart from that position and slightly moved depending on the bulk of the substituted residues. Therefore, these layers of water molecules may hardly be affected by the substitutions. In fact, the estimated $\Delta\Delta G$ of all Val 110 mutants agreed with their experimental $\Delta\Delta G$. Thus, three types of hydration structures were observed at the three positions illustrated in Figure 6. One is a fragile hydration structure (Figure 6a: Val 2). This type is easily destroyed by the substitutions. The second is a tough hydration structure (Figure 6b: Val 74). This structure tolerates the substitutions and becomes intense due to newly introduced water molecules when substituted by small residues. The third is the flexible layers of the hydration which are somewhat apart from the protein surface (Figure 6c: Val 110). Because the layers can flexibly move due to substitution, the stability is hardly affected by the substitutions.

In this study, various changes in the hydration structures could be observed, depending on the surroundings of the protein surface. Therefore, the stability of the mutant proteins whose hydration structures changed was different from the estimated stability without consideration of the hydration structures. These results suggest that the hydration structure plays an important role in determining the conformational stability of a protein. Moreover, although it is impossible to observe the hydration structures in the denatured state, the

Table 4: Contribution of Various Factors to the Stability of the Mutant Proteins Substituted at Positions 2, 74, and 110 (kJ/mol)

			$\Delta\Delta G_{HP}$			$\Delta\Delta G_{pro}$		main reason for large differences between
	$\Delta\Delta G_{exp}$	$\Delta\Delta G_{est}$	$\alpha\Delta\Delta ASA_{NP}$	$\beta\Delta\Delta ASA_{P}$	$\Delta\Delta G_{conf}$	α-helix	β-sheet	$\Delta\Delta G_{exp}$ and $\Delta\Delta G_{cal}$
V2G	−9.6	−3.2	−1.2	−0.1	−0.4		−1.5	destruction of the hydration structure
V2A	−6.3	−8.9	−7.4	0.6	−0.4		−1.7	
V2I	4.6	1.4	0.9	0.1	0.5		−0.1	
V2L	−0.2	−0.2	0.4	−0.1	0.3		−0.8	
V2M	−1.3	−3.5	−3.3	−0.5	0.9		−0.6	
V2F	−3.6	3.5	3.6	0.8	0.2		−1.1	destruction of the hydration structure
V74G	−0.9	−8.8	−9.0	0.6	−0.4			formation of a network via hydrogen bonds
V74A	−1.5	−4.7	−4.7	0.4	−0.4			
V74I	1.9	4.6	4.4	−0.3	0.5			
V74L	0.8	−2.0	−2.0	−0.2	0.2			
V74M	2.7	1.6	0.7	0.1	0.8			
V74F	−1.2	−2.5	−2.7	0.1	0.1			
V110G	2.0	−0.1	2.3	0.1	−0.2	−2.3		
V110A	2.2	0.8	−2.2	0.3	−0.2	2.9		
V110I	3.6	2.8	1.5	0.3	0.3	0.7		
V110L	0.3	1.7	−0.7	0.4	−0.3	2.3		
V110M	2.2	4.9	1.2	1.4	0.3	2.0		
V110F	−0.2	−2.5	−2.5	−0.3	−0.1	0.4		

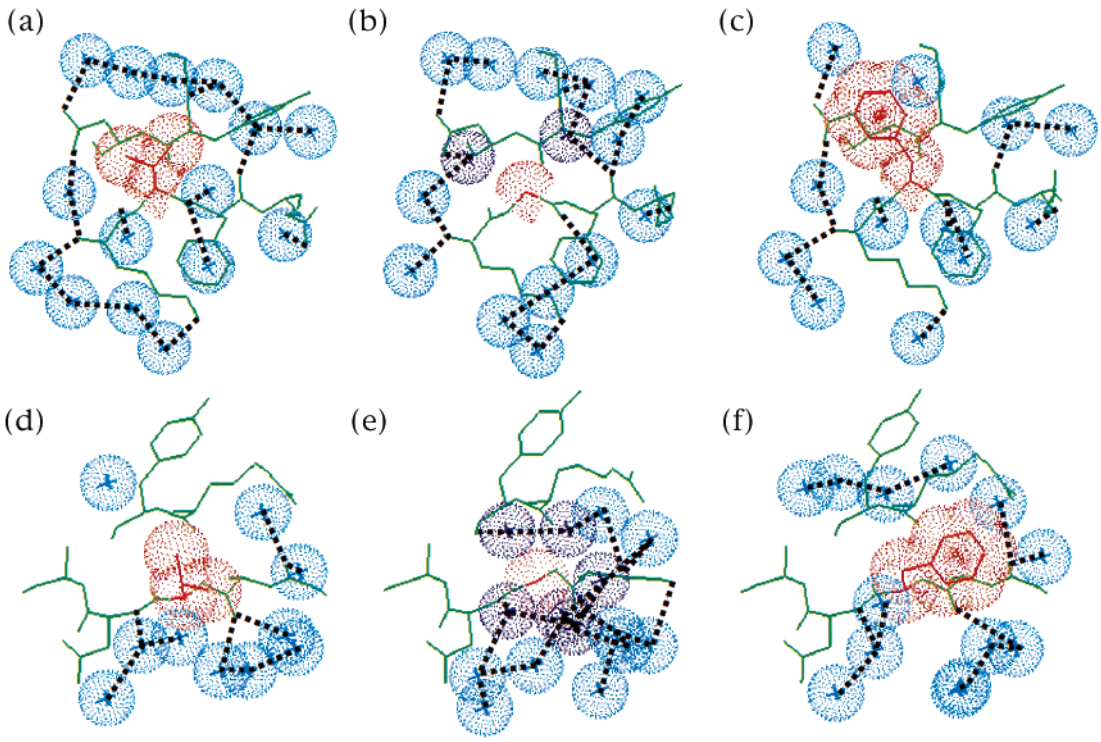

FIGURE 5: Structures in the vicinity of the substituted residue: (a) wild-type (Val 2); (b) V2G; (c) V2F; (d) wild-type (Val 74); (e) V74G; (f) V74F. Red, light blue, and blue dots represent the van der Waals surface of the substituted residue, water molecules, and water molecules introduced in the space occupied by Val in the wild-type structure, respectively. Dotted lines represent hydrogen bonds.

differences in the hydration structures between the denatured and native states should have some impact on the overall stability.

Reverse Hydrophobic Effect. Mutagenesis studies have shown that when a hydrophobic amino acid is substituted into a hyperexposed site on the surface, the protein can be destabilized, with an increase in the hydrophobicity (*5*, *7*, *8*), showing a reverse hydrophobic effect. This effect can be explained by the hydrophobic effect described in eq 5. The coefficients, 0.178 and −0.013, in eq 5 indicate the extent of stability that would be affected by increasing the nonpolar and polar surface area, respectively, due to denaturation. A nonpolar side chain that is equally exposed to the solvent in the native and denatured states should neither contribute to nor detract from stability because the change in the ΔASA_{NP} is zero. On the other hand, some nonpolar side chains may be less exposed to the solvent in the denatured state than in the native state. In this case, the protein would be destabilized because the ΔASA_{NP} is negative. This is the "reverse hydrophobic effect".

In this study, an apparent reverse hydrophobic effect was not observed (Table 3). This is because the three positions (Val 2, Val 74, and Val 110) are partly buried (28, 25, and 29%, respectively), resulting in these positions being more exposed in the denatured state than in the native state. However, the present calculation indicated that some of the Val 110 mutants might be more buried in the denatured state than in the native state. The bulky side chains, Trp 109 and

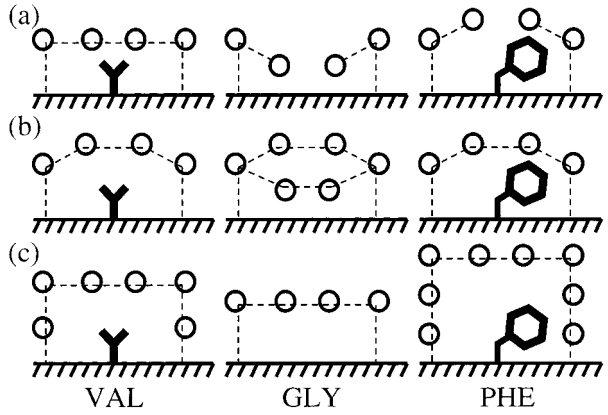

FIGURE 6: The illustration of the simplified hydration structures around positions (a) 2, (b) 74, and (c) 110. Three hydration structures in parts a, b, and c represent fragile, tough, and flexible types, respectively. Bold lines, dashed lines, and circles represent the side chains (Val, Gly, and Phe) at each position, the hydrogen bonds, and water molecules, respectively.

Trp 112, near position 110 can decrease the surface area of position 110 in the denatured state. This suggests that it is essential to determine the structure of the denatured state precisely in order to estimate the conformational stability of a protein.

CONCLUSIONS

In the present study, three exposed positions which are located in the α-helix, the β-sheet, and the loop were replaced by a series of hydrophobic residues. Using the parameters of the contribution of the stabilization factors, newly considering the propensity of the secondary structure, the stability of the mutant proteins substituted at the surface positions could be estimated. Although these three positions are located in different environments on the structure, the estimated values coincided with the experimental values except for V2G, V2F, and V74G. The differences between $\Delta\Delta G_{exp}$ and $\Delta\Delta G_{est}$ of these mutant proteins would be explained by destruction (V2G and V2F) or formation (V74G) of the hydration structure around the mutation sites, suggesting that the hydration structure plays an important role in determining the conformational stabilities of a protein. This is the first case in which stability changes due to the changes in the hydration structures were observed. We are studying a series of hydrophilic mutants on the surface of human lysozyme as our next project.

ACKNOWLEDGMENT

We thank Professor M. Nakasako (The University of Tokyo) for helpful advice and useful discussions. We also thank Takeda Chemical Industries (Osaka) for providing plasmid pGEL 125.

REFERENCES

1. Reidhaar-Olson, J. F., and Sauer, R. T. (1988) *Science 241*, 53−57.
2. Bowie, J. U., Reidhaar-Olson, J. F., Lim, W. A., and Sauer, R. T. (1990) *Science 247*, 1306−1310.
3. Rennell, D., Bouvier, S. E., Hardy, L. W., and Poteete, A. R. (1991) *J. Mol. Biol. 222*, 67−88.
4. Schwehm, J. M., Kristyanne, E. S., Biggers, C. C., and Stites, W. E. (1998) *Biochemistry 37*, 6939−6948.
5. Pakula, A. A., and Sauer, R. T. (1990) *Nature 344*, 363−364.
6. Burg, B. V. D., Dijkstra, B. W., Vriend, G., Vinne, B. V. D., Venema, G., and Eijsink, V. G. H. (1994) *Eur. J. Biochem. 220*, 981−985.
7. Herrmann, L., Bowler, B. E., Dong, A., and Caughey, W. S. (1995) *Biochemistry 34*, 3040−3047.
8. Tamura, A., and Sturtevant, J. M. (1995) *J. Mol. Biol. 249*, 646−653.
9. Cordes, M. H. J., and Sauer, R. T. (1999) *Protein Sci. 8*, 318−325.
10. Perl, D., Mueller, U., Heinemann, U., and Schmid, F. X. (2000) *Nat. Struct. Biol. 7*, 380−383.
11. Tisi, L. C., and Evans, P. A. (1995) *J. Mol. Biol. 249*, 251−258.
12. Takano, K., Ogasahara, K., Kaneda, H., Yamagata, Y., Fujii, S., Kanaya, E., Kikuchi, M., Oobatake, M., and Yutani, K. (1995) *J. Mol. Biol. 254*, 62−76.
13. Nagata, C., Moriyama, H., Tanaka, N., Nakasako, M., Yamamoto, M., Ueki, M., and Oshima, T. (1996) *Acta Crystallogr. D52*, 623−630.
14. Nakasako, M. (1999) *J. Mol. Biol. 289*, 547−564.
15. Parry, R. M., Chandan, R. C., and Shahani, K. M. (1969) *Arch. Biochem. Biophys. 130*, 59−65.
16. Yamagata, Y., Kubota, M., Sumikawa, Y., Funahashi, J., Takano, K., Fujii, S., and Yutani, K. (1998) *Biochemistry 37*, 9355−9362.
17. Brunger, A. T. (1992). *X-PLOR Manual*, version 3.1, Yale University, New Haven, CT.
18. Takano, K., Yamagata, Y., Fujii, S., and Yutani, K. (1997) *Biochemistry 36*, 688−698.
19. Connolly, M. L. (1993) *J. Mol. Graphics 11*, 139−141.
20. Takano, K., Yamagata, Y., and Yutani, K. (1998) *J. Mol. Biol. 280*, 749−761.
21. Funahashi, J., Takano, K., Yamagata, Y., and Yutani, K. (1999) *Protein Eng. 12*, 841−850.
22. Oobatake, M., and Ooi, T. (1993) *Prog. Biophys. Mol. Biol. 59*, 237−284.
23. Privalov, P. L., and Khechinashvili, N. N. (1974) *J. Mol. Biol. 86*, 665−684.
24. Takano, K., Funahashi, J., Yamagata, Y., Fujii, S., and Yutani, K. (1997) *J. Mol. Biol. 274*, 132−142.
25. Takano, K., Yamagata, Y., Kubota, M., Funahashi, J., Fujii, S., and Yutani, K. (1999) *Biochemistry 38*, 6623−6629.
26. Takano, K., Yamagata, Y., Funahashi, J., Hioki, Y., Kuramitsu, S., and Yutani, K. (1999) *Biochemistry 38*, 12698−12708.
27. Takano, K., Ota, M., Ogasahara, K., Yamagata, Y., Nishikawa, K., and Yutani, K. (1999) *Protein Eng. 12*, 663−672.
28. Funahashi, J., Takano, K., Ogasahara, K., Yamagata, Y., and Yutani, K. (1996) *J. Biochem. (Tokyo) 120*, 1216−1223.
29. Pace, C. N., and Scholtz, J. M. (1998) *Biophys. J. 75*, 422−427.
30. Ibarra-Molero, B., Loladze, V. V., Makhatadze, G. I., and Sanchez-Ruiz, J. M. (1999) *Biochemistry 38*, 8138−8149.
31. Eriksson, A. E., Baase, W. A., Zhang, X.-J., Heinz, D. W., Blaber, M., Baldwin, E. P., and Matthews, B. W. (1992) *Science 225*, 178−183.
32. Pace, C. N. (1992) *J. Mol. Biol. 226*, 29−35.
33. Serrano, L., Kellis, J. T., Cann, P., Matouschek, A., and Fersht, A. R. (1992) *J. Mol. Biol. 224*, 783−804.
34. Shirley, B. A., Stanssens, P., Hahn, U., and Pace, C. N. (1992) *Biochemistry 31*, 725−732.
35. Buckle, A. M., Henrick, K., and Fersht, A. R. (1993) *J. Mol. Biol. 234*, 847−860.
36. Byrne, P. M., Manuel, R. L., Lowe, L. G., and Stites, W. E. (1995) *Biochemistry 34*, 13949−13960.
37. Yu, M.-H., Weissman, J. S., and Kim, P. S. (1995) *J. Mol. Biol. 249*, 388−397.
38. Myers, J. K., and Pace, C. N. (1996) *Biophys. J. 71*, 2033−2039.
39. Pace, C. N., Shirley, B. A., Mcnutt, M., and Gajiwala, K. (1996) *FASEB J. 10*, 75−83.
40. Xu, J., Baase, W. A., Baldwin, E., and Matthews, B. W. (1998) *Protein Sci. 7*, 158−177.
41. Doig, A. J., and Sternberg, M. J. E. (1995) *Protein Sci. 4*, 2247−2251.

42. Creamer, T. P., and Rose, G. D. (1994) *Proteins: Struct., Funct., Genet. 19*, 85−97.
43. Chou, P. Y., and Fasman, G. D. (1978) *Adv. Enzymol. Relat. Areas Mol. Biol. 47*, 45−148.
44. Koehl, P., and Levitt, M. (1999) *Proc. Natl. Acad. Sci. U.S.A. 96*, 12524−12529.
45. Lyu, P. C., Liff, M. L., Markey, L. A., and Kallenbach, N. R. (1990) *Science 250*, 669−673.
46. O'Neil, K. T., and DeGrado, W. F. (1990) *Science 250*, 646−651.
47. Blaber, M., Zhang, X. J., Lindstrom, J. D., Pepiot, S. D., Baase, W. A., and Matthews, B. W. (1994) *J. Mol. Biol. 235*, 600−624.
48. Kim, C. A., and Berg, J. M. (1993) *Nature 362*, 267−270.
49. Minor, D. L., and Kim, P. S. (1994) *Nature 367*, 660−663.
50. Minor, D. L., and Kim, P. S. (1994) *Nature 371*, 264−267.
51. Smith, C. K., Withka, J. M., and Regan, L. (1994) *Biochemistry 33*, 5510−5517.

BI0015717